

Table 6-1. Uranium decay series

Uranium 238			Uranium 235		
Isotope	Emitted particle	Half-life	Isotope	Emitted particle	Half-life
$^{238}_{92}\text{U}$	α	4.47 x 10 ⁹ yrs	$^{235}_{92}\text{U}$	α	7.038 x 10 ⁸ yrs
$^{234}_{90}\text{Th}$	β^-	24.1 days	$^{231}_{90}\text{Th}$	β^-	1.063 days
$^{234}_{91}\text{Pa}$	β^-	1.17 min	$^{231}_{91}\text{Pa}$	α	3.248 x 10 ⁴ yrs
$^{234}_{92}\text{U}$	α	2.48 x 10 ⁵ yrs	$^{227}_{89}\text{Ac}$	β^-	21.77 yrs
$^{230}_{90}\text{Th}$	α	7.52 x 10 ⁴ yrs	$^{227}_{90}\text{Th}$	α	18.72 days
$^{226}_{88}\text{Ra}$	α	1.60 x 10 ³ yrs	$^{223}_{88}\text{Ra}$	α	11.435 days
$^{222}_{86}\text{Rn}$	α	3.8235 days	$^{219}_{86}\text{Rn}$	α	3.96 sec
$^{218}_{84}\text{Po}$	α	3.10 min	$^{215}_{84}\text{Po}$	α	1.78 x 10 ⁻³ sec
$^{214}_{82}\text{Pb}$	β^-	27 min	$^{211}_{82}\text{Pb}$	β^-	36.1 min
$^{214}_{83}\text{Bi}$	β^-	19.9 min	$^{211}_{83}\text{Bi}$	α	2.14 min
$^{214}_{84}\text{Po}$	α	1.64 x 10 ⁻⁴ sec	$^{207}_{81}\text{Tl}$	β^-	4.77 min
$^{210}_{82}\text{Pb}$	β^-	22.3 yrs	$^{207}_{82}\text{Pb}$		Stable
$^{210}_{83}\text{Bi}$	β^-	5.01 days			
$^{210}_{84}\text{Po}$	α	138.38 days			
$^{206}_{82}\text{Pb}$		Stable			

Table 6-2. Thorium decay series

Isotope	Emitted particle	Half-life	Isotope	Emitted particle	Half-life
$^{232}_{90}\text{Th}$	α	1.40×10^{10} yrs	$^{216}_{84}\text{Po}$	α	0.145 sec
$^{228}_{88}\text{Ra}$	β^-	5.76 yrs	$^{212}_{82}\text{Pb}$	β^-	10.64 hr
$^{228}_{89}\text{Ac}$	β^-	6.15 hr	$^{212}_{83}\text{Bi}$	α (33.7%) β^- (66.3%)	1.009 hr
$^{228}_{90}\text{Th}$	α	1.913 yrs	$^{208}_{81}\text{Tl}$	β^-	3.053 min
$^{224}_{88}\text{Ra}$	α	3.66 days	$^{212}_{84}\text{Po}$	α	2.98×10^{-7} sec
$^{220}_{86}\text{Rn}$	α	55.6 sec	$^{208}_{82}\text{Pb}$		Stable

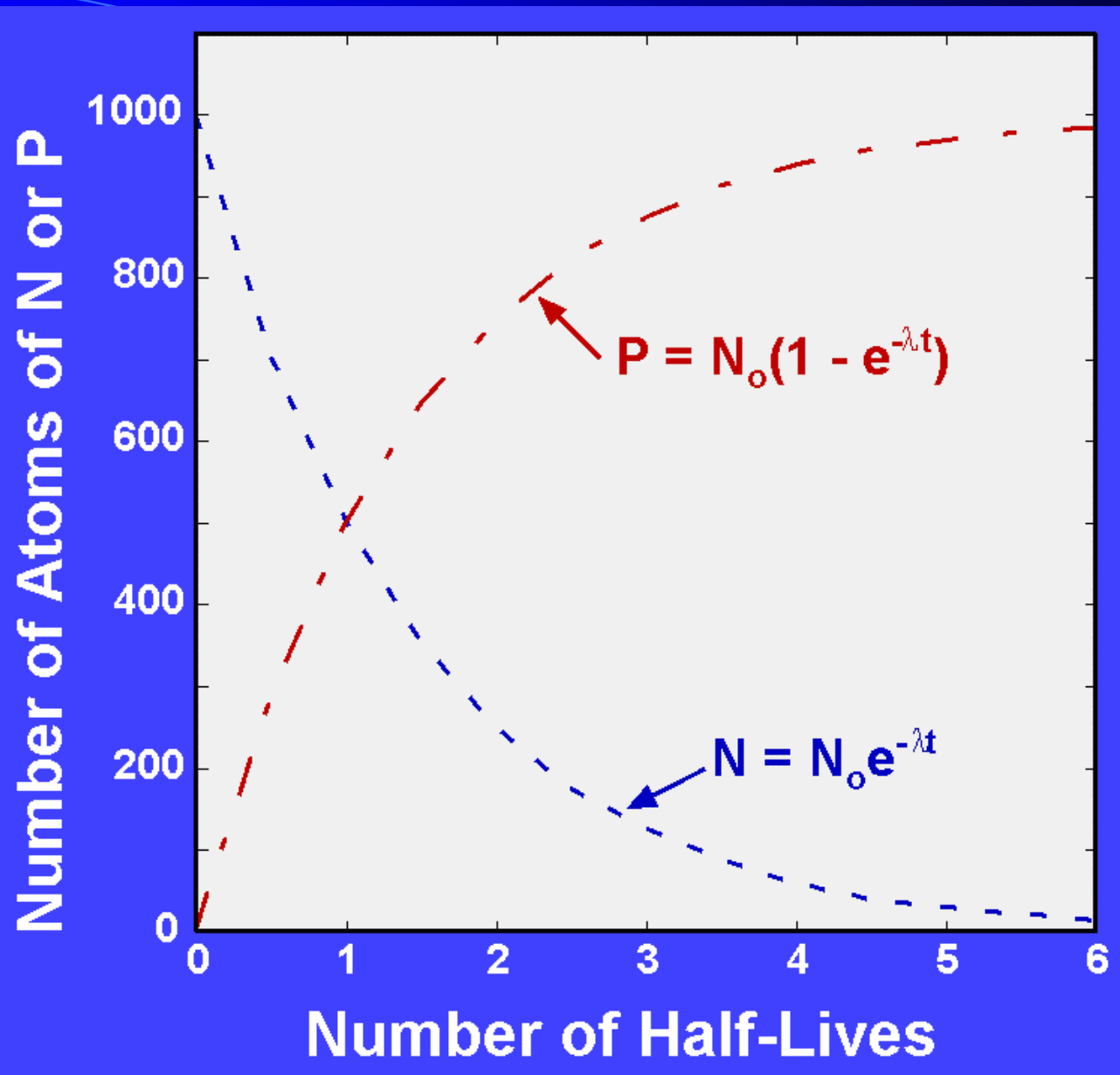


Figure 6-1. Graphical representation of decay of radioactive parent (N) and growth of radiogenic progeny (P).

Table 6-3. RBE values for various types of radiation

Radiation	RBE
X and γ rays	1
Beta rays and electrons	1
Thermal neutrons	2
Fast neutrons	10
Protons	10
Alpha particles	20
Heavy ions	20

Table 6-4. Radiometric isotopes used in environmental studies

Radioactive parent	Radiogenic progeny	Type of Decay	Half-life (years)	Decay constant (y^{-1})
${}^3_1\text{H}$	${}^3_2\text{He}$	β^-	12.43	5.575×10^{-2}
${}^{14}_6\text{C}$	${}^{14}_7\text{N}$	β^-	5.73×10^3	1.209×10^{-4}
${}^{36}_{17}\text{Cl}$	${}^{36}_{18}\text{Ar}$	β^-	3.01×10^5	2.302×10^{-6}
${}^{81}_{36}\text{Kr}$	${}^{81}_{35}\text{Br}$	ϵ	2.10×10^5	3.300×10^{-6}
${}^{234}_{92}\text{U}$	${}^{230}_{90}\text{Th}$	α	2.48×10^5	2.794×10^{-6}
${}^{230}_{90}\text{Th}$	${}^{226}_{88}\text{Ra}$	α	7.52×10^4	9.217×10^{-6}
${}^{226}_{88}\text{Ra}$	${}^{222}_{84}\text{Rn}$	α	1.622×10^3	4.272×10^{-4}
${}^{210}_{82}\text{Pb}$	${}^{210}_{83}\text{Bi}$	β^-	22.26	3.11×10^{-2}
${}^{231}_{91}\text{Pa}$	${}^{227}_{89}\text{Ac}$	α	3.248×10^4	2.134×10^{-5}
${}^{37}_{87}\text{Rb}$	${}^{38}_{87}\text{Sr}$	β^-	4.88×10^{10}	1.42×10^{-11}
${}^{232}_{90}\text{Th}$	${}^{208}_{82}\text{Pb}$	α, β^-	1.401×10^{10}	4.948×10^{-11}
${}^{235}_{92}\text{U}$	${}^{207}_{82}\text{Pb}$	α, β^-	7.038×10^8	9.849×10^{-10}
${}^{238}_{92}\text{U}$	${}^{206}_{82}\text{Pb}$	α, β^-	4.468×10^9	1.551×10^{-10}

Table 6-5. Calculation of $^{230}\text{Th}/^{232}\text{Th}$ for unsupported and supported ^{230}Th and total ^{230}Th

Age 10 ⁵ years	$^{230}\text{Th}/^{232}\text{Th}$ Ratio		
	Unsupported	Supported	Observed
0	42	0	42
1	16.7	1.20	17.9
2	6.65	1.68	8.33
3	2.64	1.87	4.51
4	1.05	1.95	3.00
5	0.42	1.98	2.40
6	0.17	1.99	2.16
7	0.07	2.00	2.07
8	0.03	2.00	2.03
9	0.01	2.00	2.01
10	0	2.00	2.00

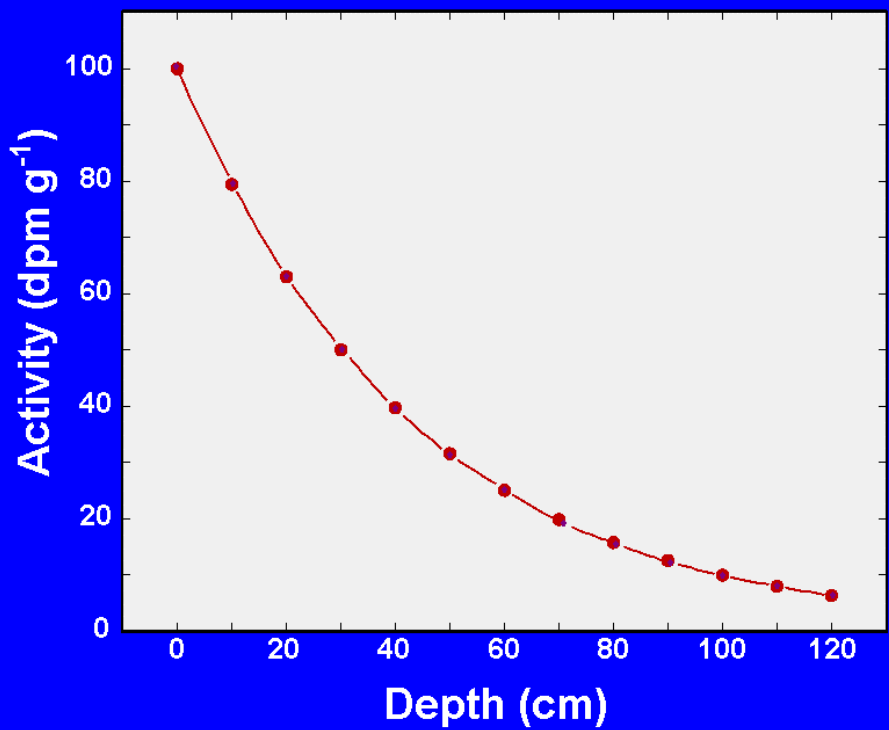


Figure 6-2. Variation of activity with depth at a constant sedimentation rate. Because radioactive decay is a first-order reaction, the data define a curved line.

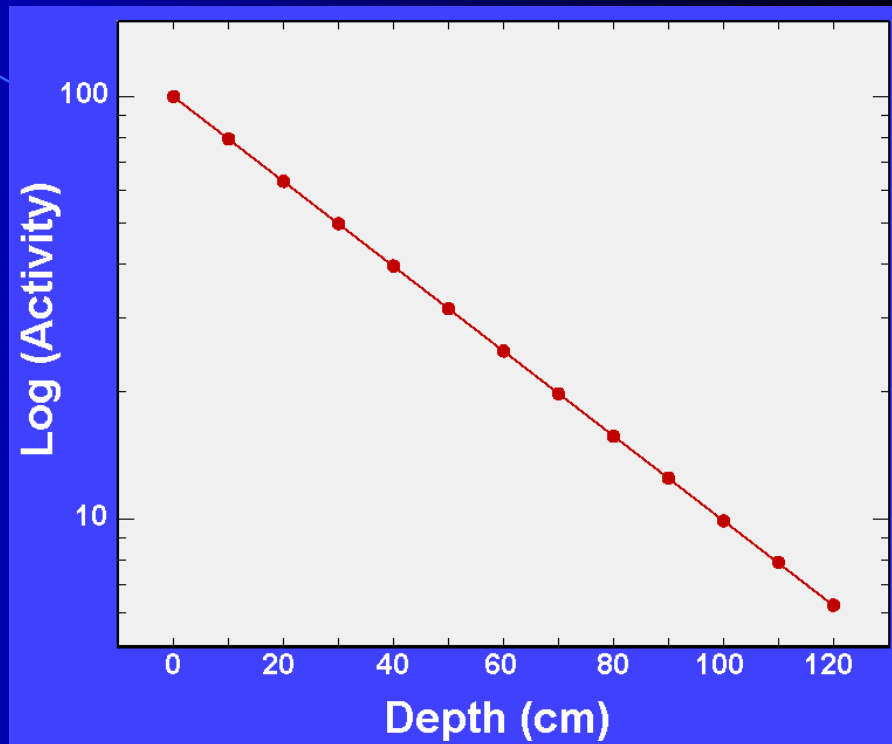


Figure 6-3. Plot of log activity versus depth (arithmetic). For a constant sedimentation rate, the data define a straight line and the sedimentation rate can be determined from the slope of the line (see text). In this case $m = -0.01003$. If $\lambda = 9.24 \times 10^{-6}$, the sedimentation rate (a) is 4×10^{-4} cm/y = 0.4 cm/1000 y.

Table 6-6. Average terrestrial abundances of stable isotopes used in environmental studies

Element	Isotope	Average Terrestrial Abundance (atom %)
Hydrogen	^1_1H	99.985
	^2_1H	0.015
Carbon	$^{12}_6\text{C}$	98.9
	$^{13}_6\text{C}$	1.1
Nitrogen	$^{14}_7\text{N}$	99.63
	$^{15}_7\text{N}$	0.37
Oxygen	$^{16}_8\text{O}$	99.762
	$^{17}_8\text{O}$	0.038
	$^{18}_8\text{O}$	0.2
Sulfur	$^{32}_{16}\text{S}$	95.02
	$^{33}_{16}\text{S}$	0.75
	$^{34}_{16}\text{S}$	4.21
	$^{36}_{16}\text{S}$	0.014

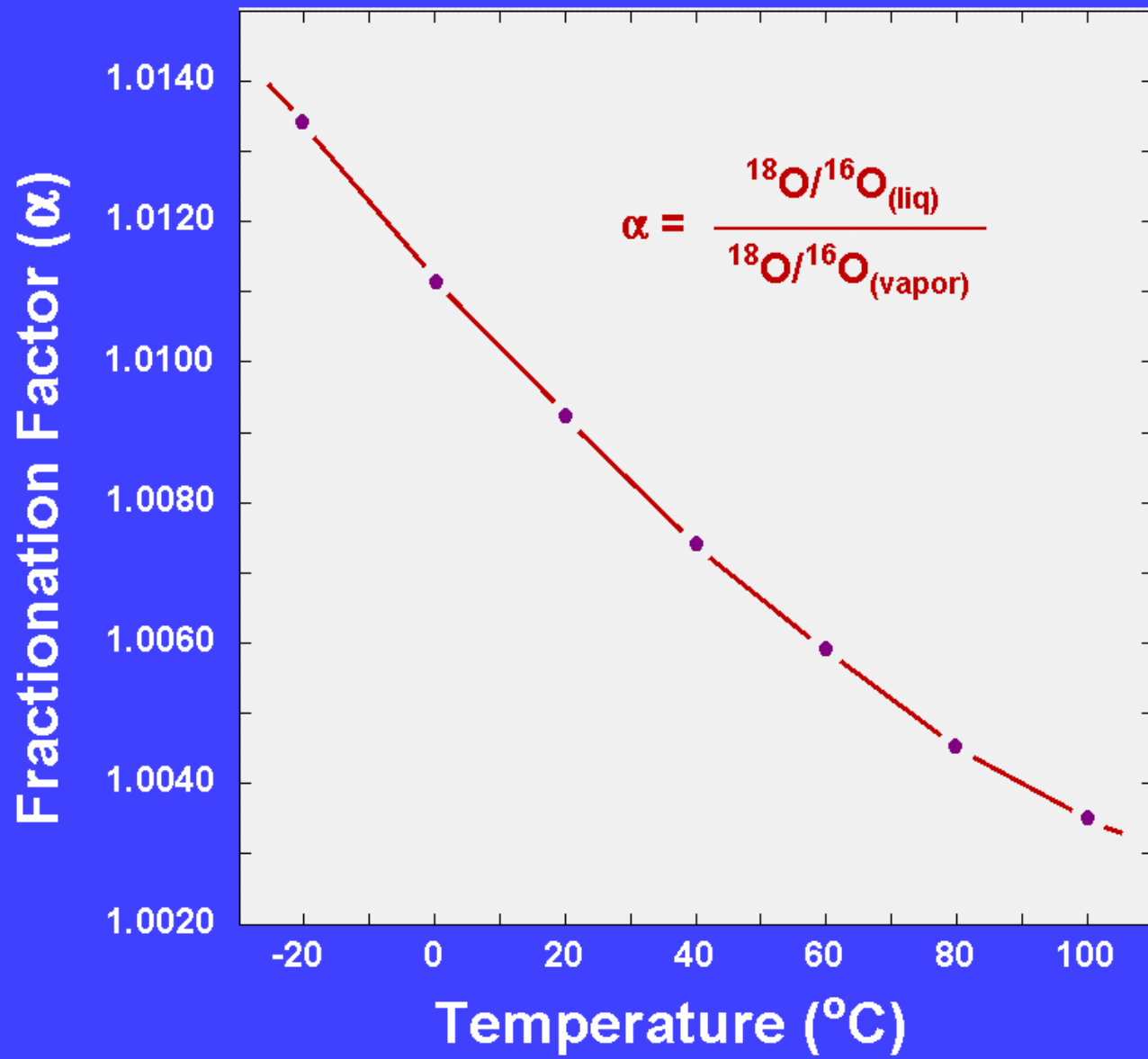


Figure 6-4. Variation of the isotope fractionation factor for oxygen, as a function of temperature, during the evaporation of water. Note that with increasing temperature the fractionation factor approaches 1.0000. Values from Dansgaard (1964).

Table 6-7. Stable isotope ratios for standards

Element	Standard	Ratio
Hydrogen	V-SMOW	$^2\text{H}/^1\text{H} = 155.76 \times 10^{-6}$
Carbon	PDB	$^{13}\text{C}/^{12}\text{C} = 1123.75 \times 10^{-5}$
Oxygen	V-SMOW	$^{18}\text{O}/^{16}\text{O} = 2005.2 \times 10^{-6}$
	PDB	$^{18}\text{O}/^{16}\text{O} = 2067.2 \times 10^{-6}$
Nitrogen	NBS-14	$^{15}\text{N}/^{14}\text{N} = 367.6 \times 10^{-5}$
Sulfur	CDT	$^{34}\text{S}/^{32}\text{S} = 449.94 \times 10^{-4}$

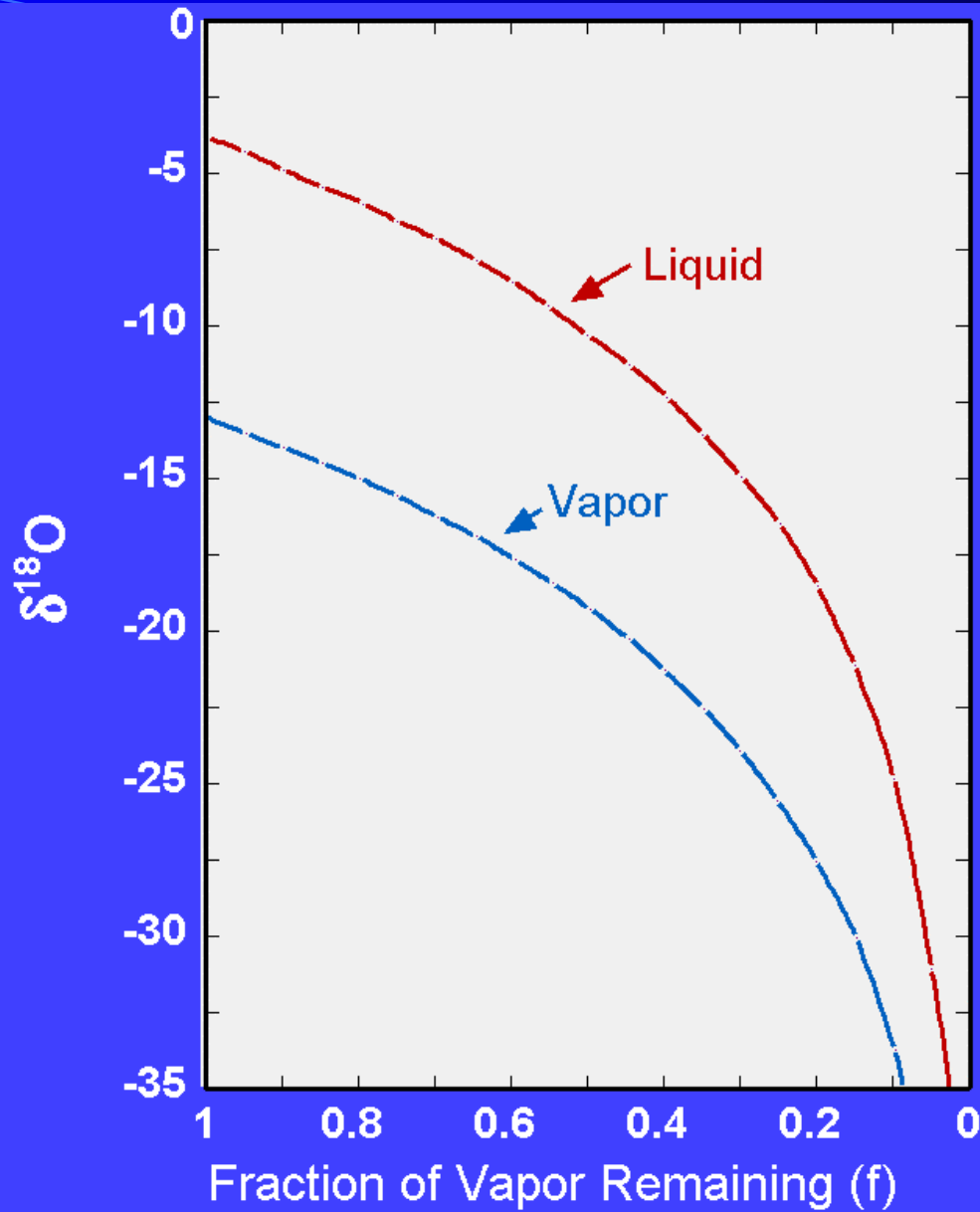


Figure 6-5. Fractionation of oxygen isotopes during Rayleigh distillation of water vapor at 25°C. The initial $\delta^{18}\text{O}$ value of the vapor is -13‰ .

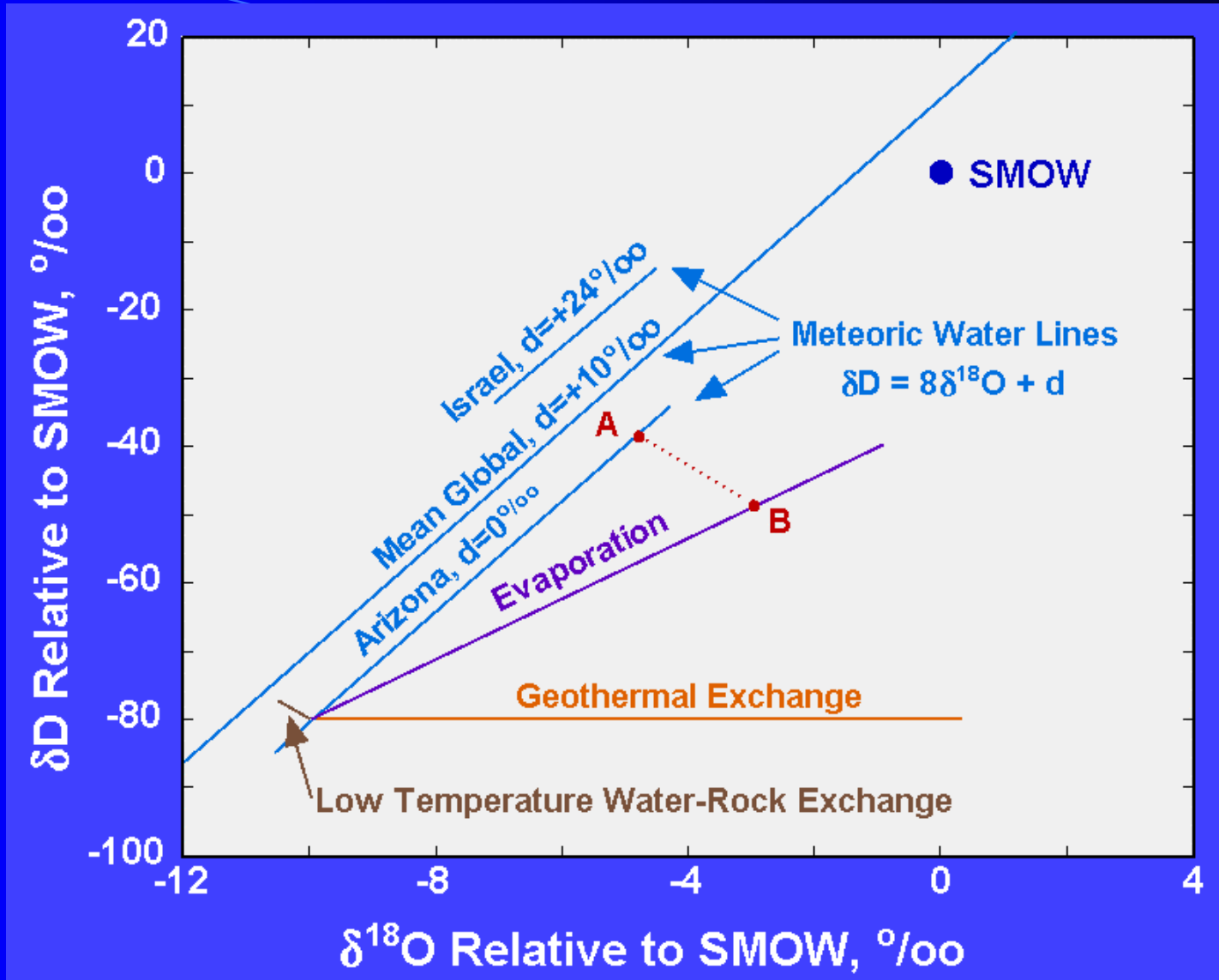


Figure 6-6. Plot of δD versus $\delta^{18}O$ illustrating the mean global meteoric water line and local meteoric water lines.

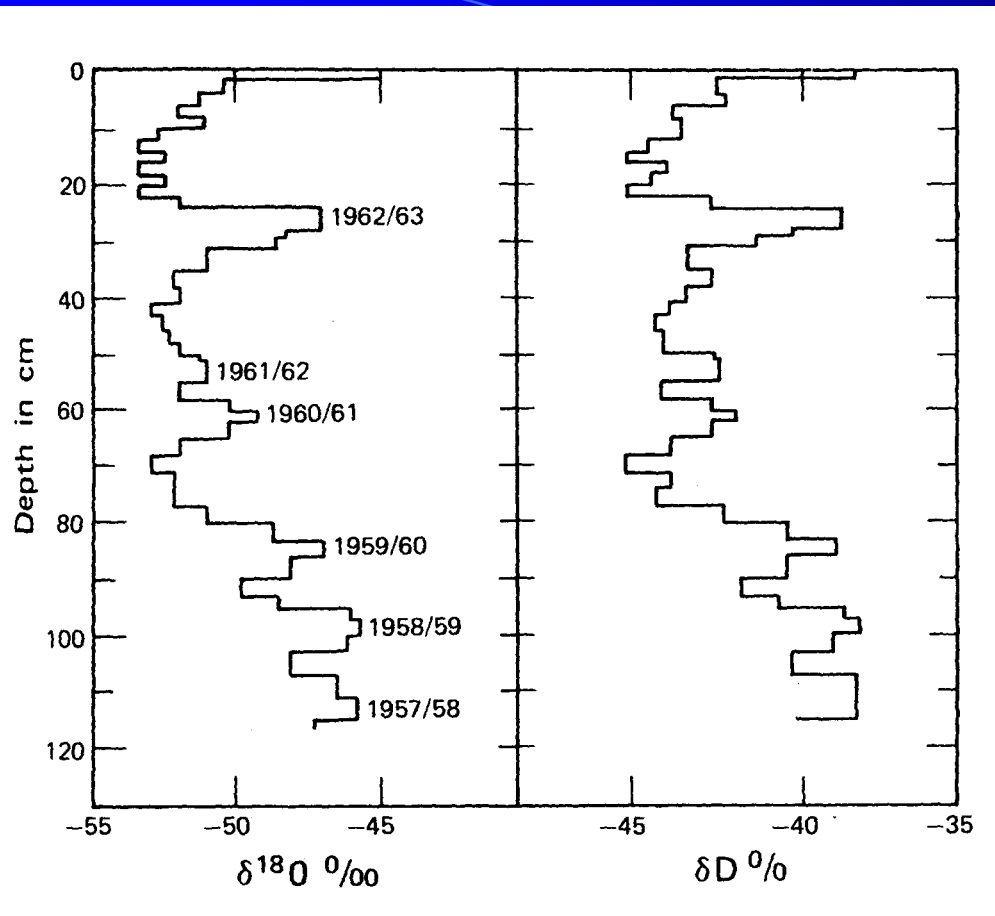


Figure 6-7. Seasonal variations in $\delta^{18}\text{O}$ and δD in snow and firn at the south pole. From PRINCIPLES OF ISOTOPE GEOLOGY, 2nd Edition by G. Faure. Copyright 1986. This material is used by permission of John Wiley & Sons, Inc.

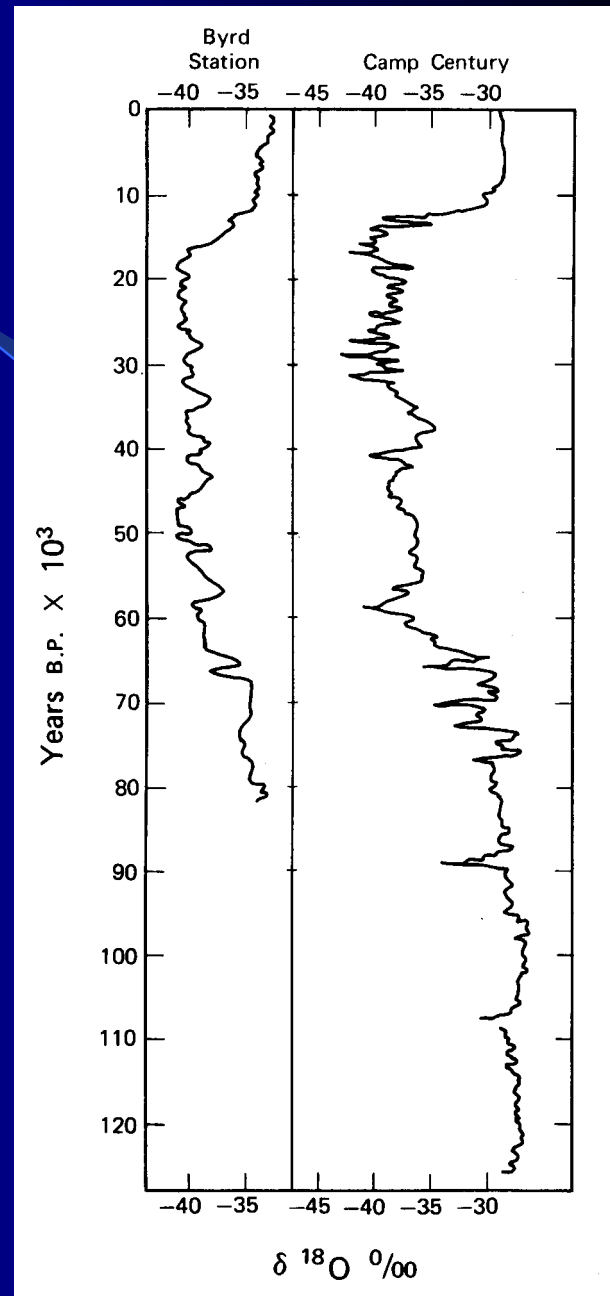


Figure 6-8. Variations in $\delta^{18}\text{O}$ from Byrd Station and Camp Century. From PRINCIPLES OF ISOTOPE GEOLOGY, 2nd Edition by G. Faure. Copyright 1986. This material is used by permission of John Wiley & Sons, Inc.

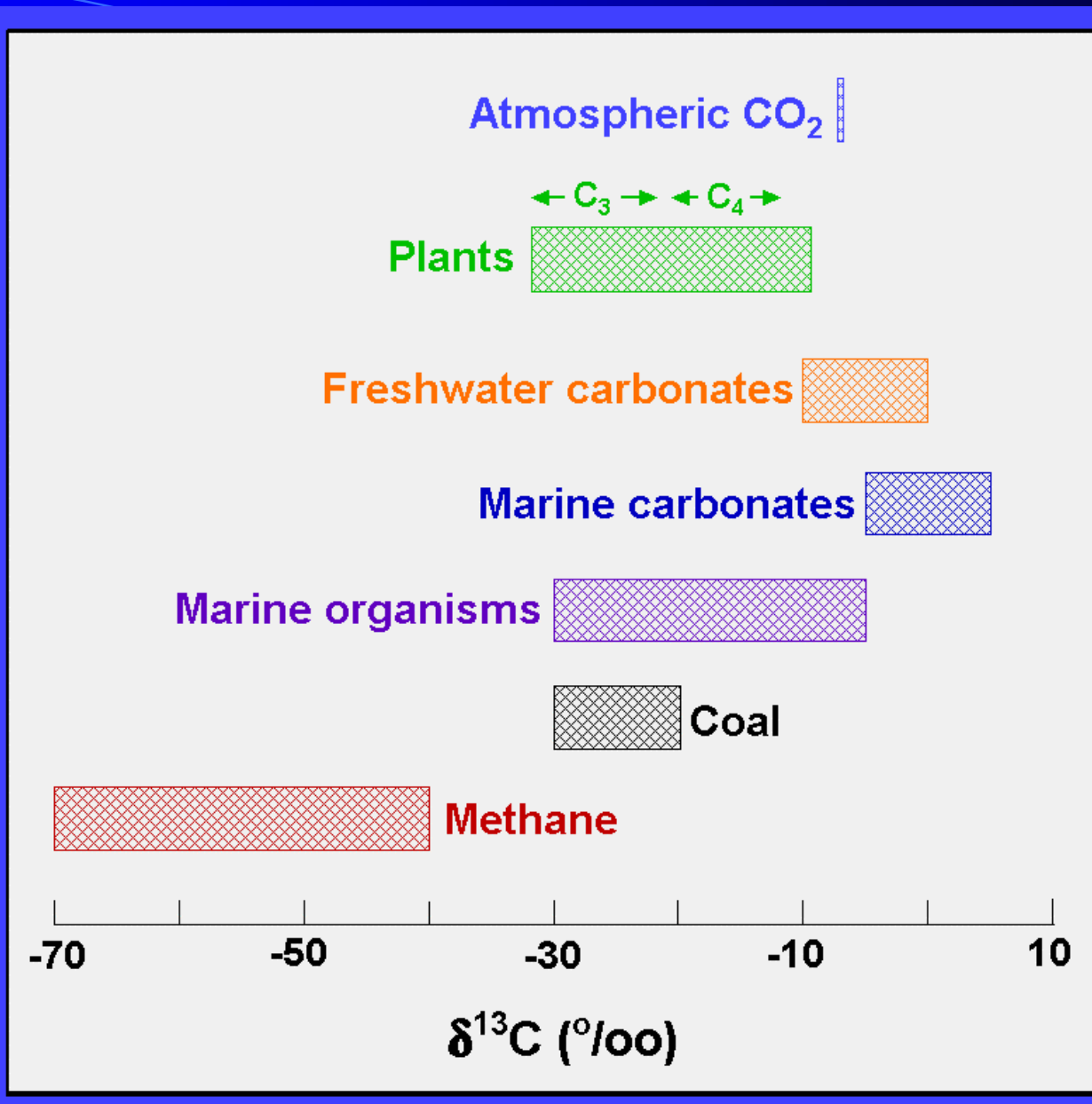


Figure 6-9. Range of $\delta^{13}\text{C}$ values for different carbon reservoirs.

Table 6-8. Fractionation factors for carbonate species relative to gaseous CO₂

H ₂ CO ₃	$1000 \ln \alpha = -0.91 + 0.0063 \cdot 10^6/T^2$
HCO ₃ ⁻	$1000 \ln \alpha = -4.54 + 1.099 \cdot 10^6/T^2$
CO ₃ ²⁻	$1000 \ln \alpha = -3.4 + 0.87 \cdot 10^6/T^2$
CaCO _{3(s)}	$1000 \ln \alpha = -3.63 + 1.194 \cdot 10^6/T^2$

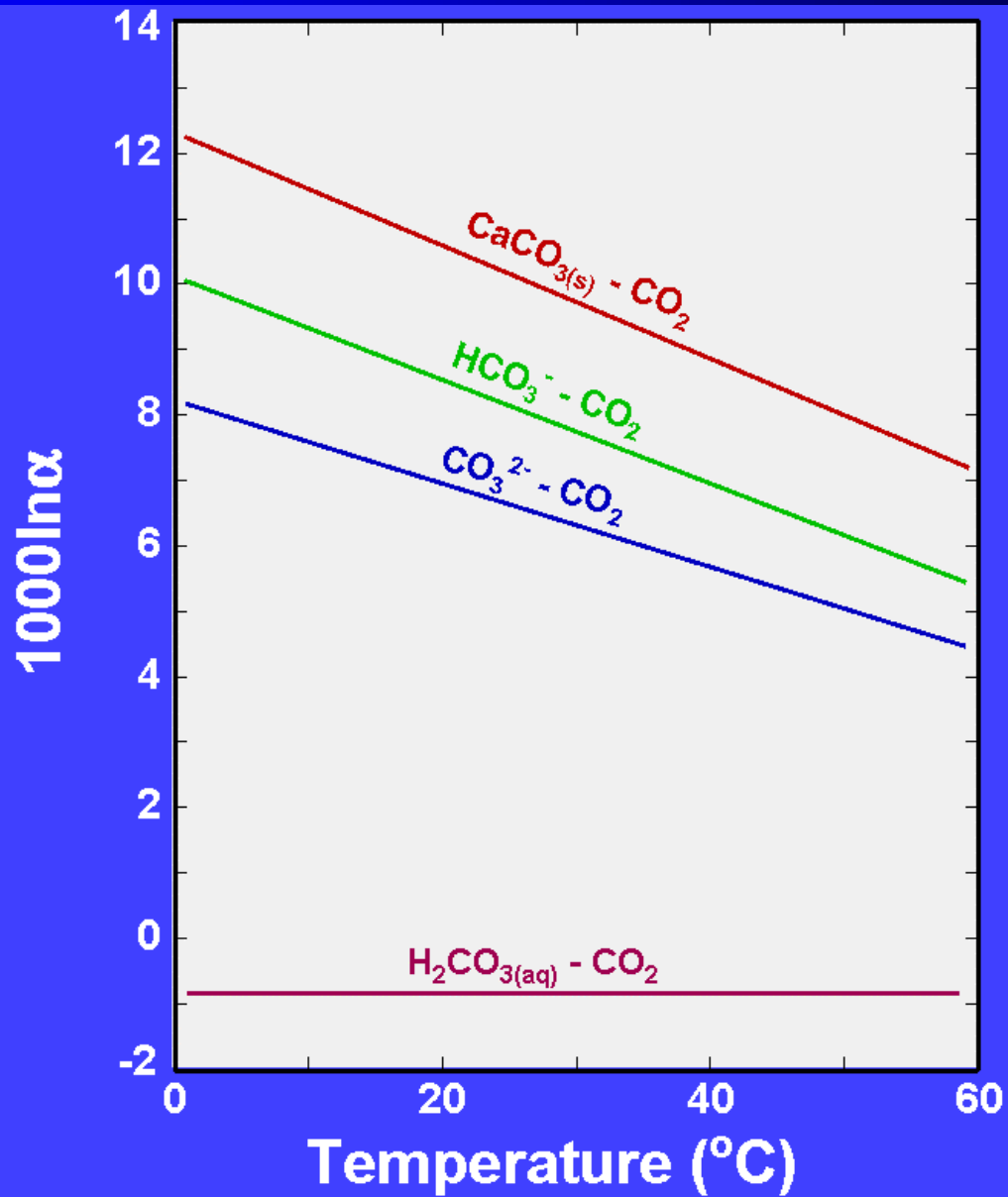


Figure 6-10. Isotope fractionation factors, relative to CO_2 gas, for carbonate species as a function of temperature. Deines et al. (1974).

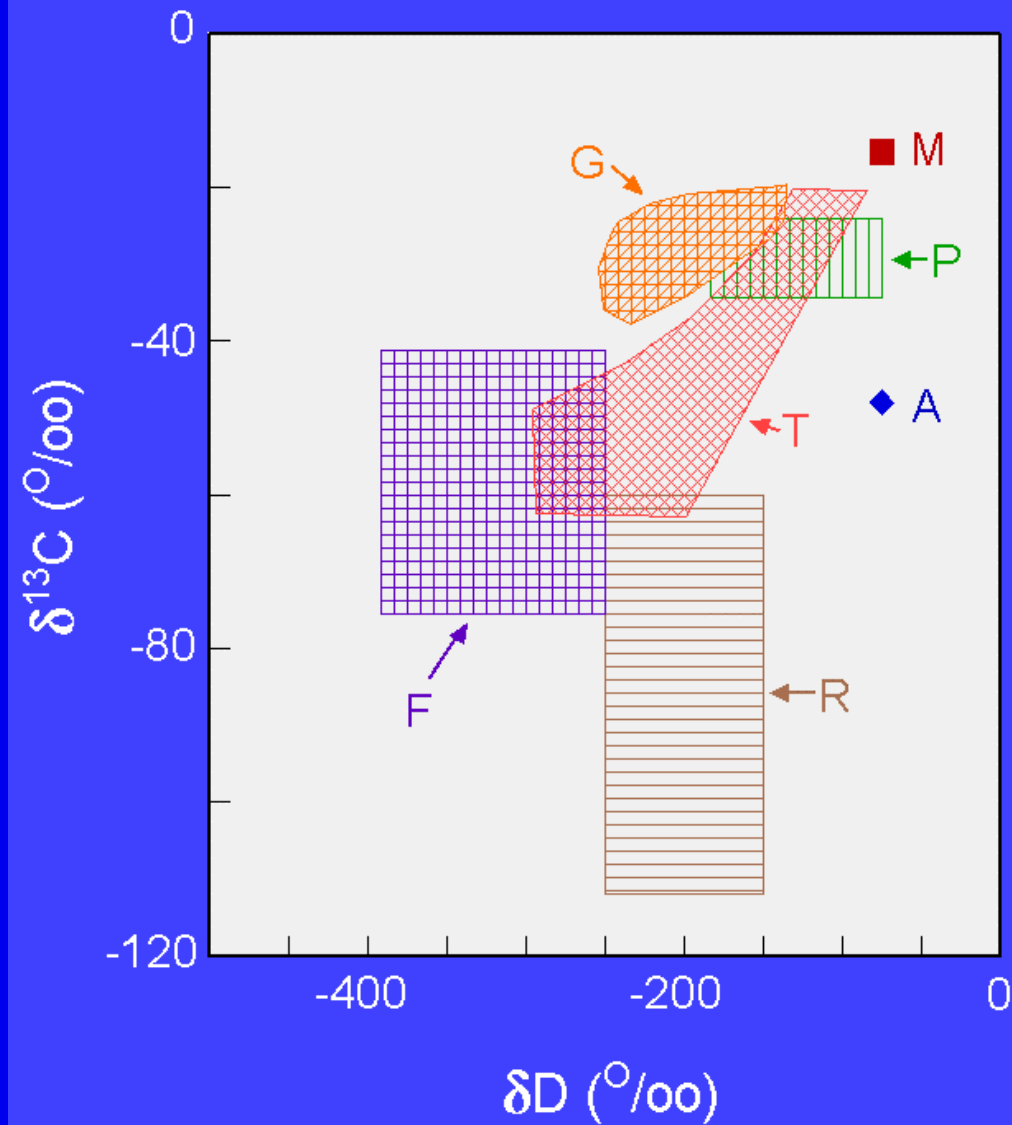


Figure 6-11. ^{13}C and deuterium isotopic values for methane from various sources and reservoirs. P – petroleum, A – atmosphere, G – geothermal (pyrolytic from interaction with magmatic heat), T – thermogenic (from kerogen at elevated temperatures), F – acetate fermentation (bacterial), and R – CO_2 reduction (bacterial). After Schoell (1984, 1988).

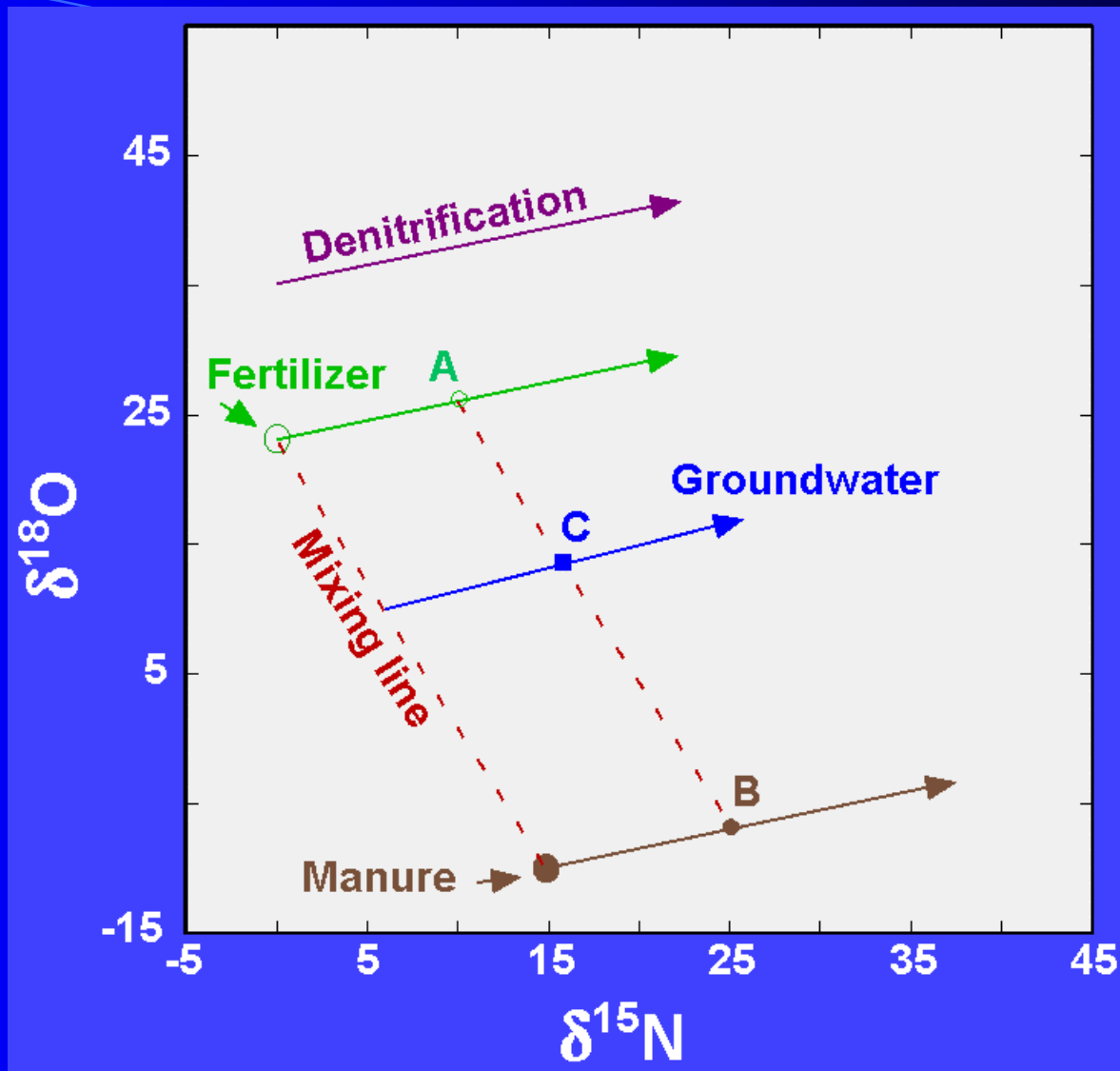


Figure 6-12. Determination of the relative importance of nitrate sources to a groundwater system. Two sources for nitrates are fertilizer and manure. Both are undergoing denitrification. A and B represent each source at a particular stage in the denitrification process. C is the isotopic composition of the nitrate in the groundwater due to simple mixing. In this example, approximately 60% of the nitrate is contributed by the fertilizer.

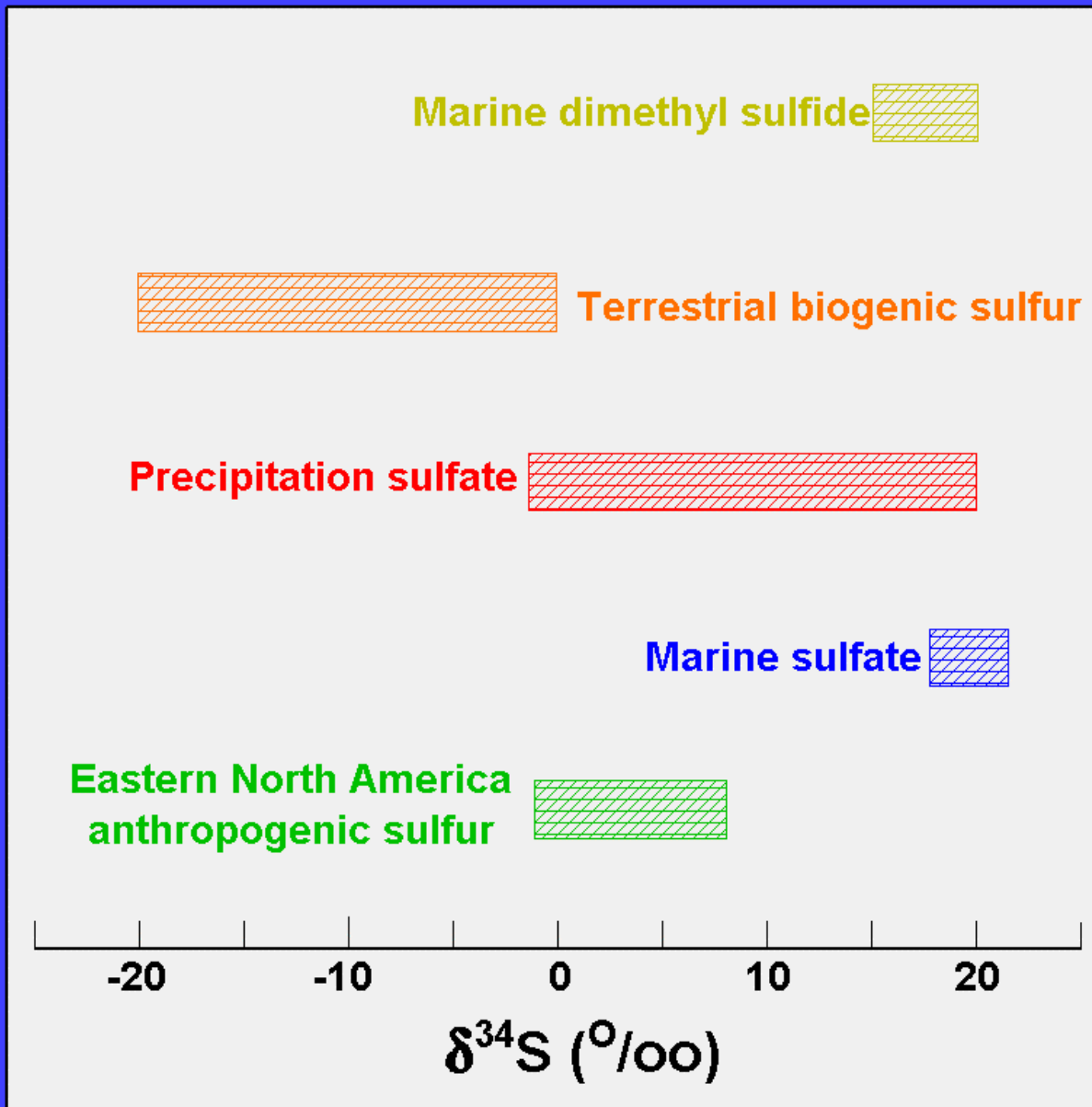


Figure 6-13. Range of $\delta^{34}\text{S}$ values for sulfur sources that contribute to atmospheric sulfur.

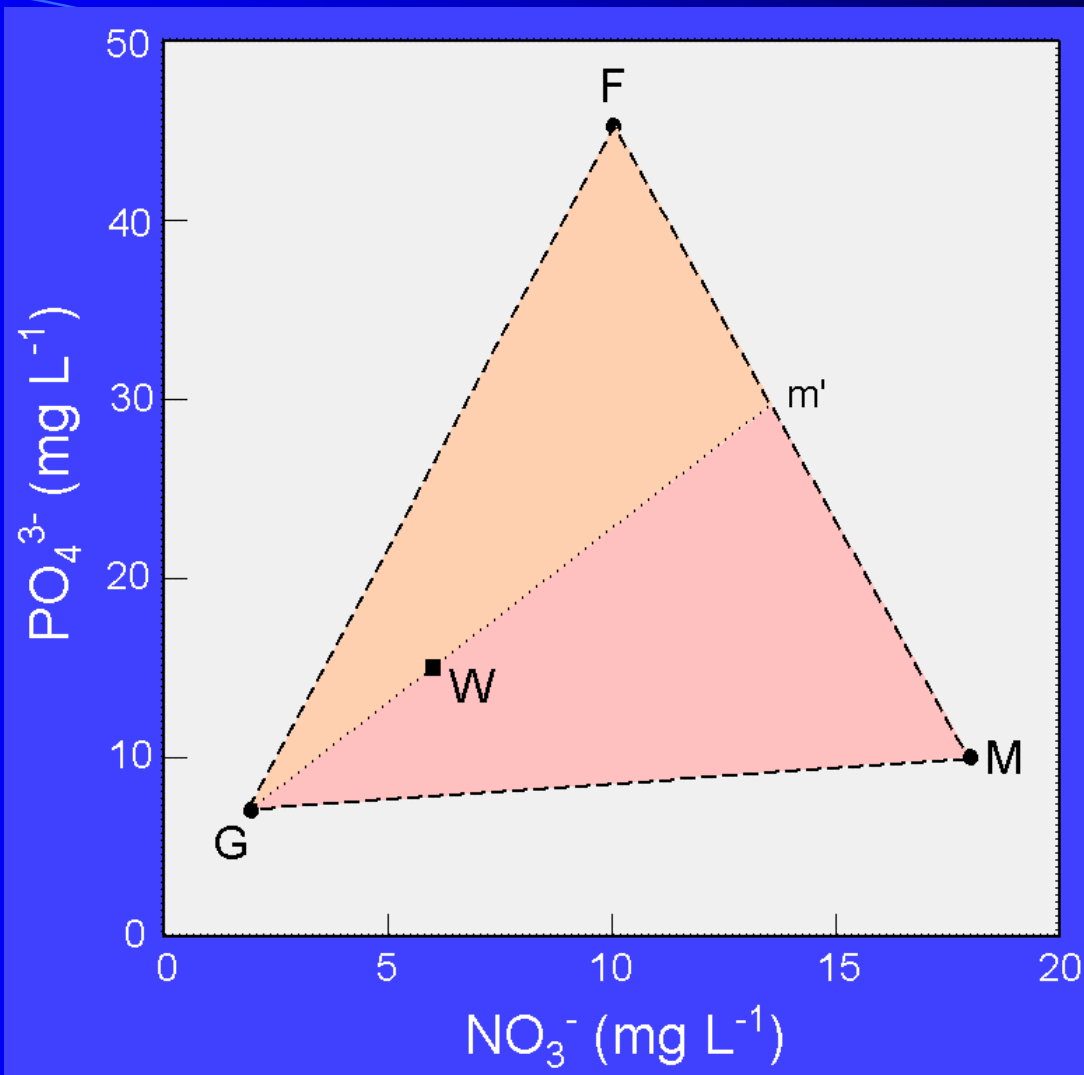
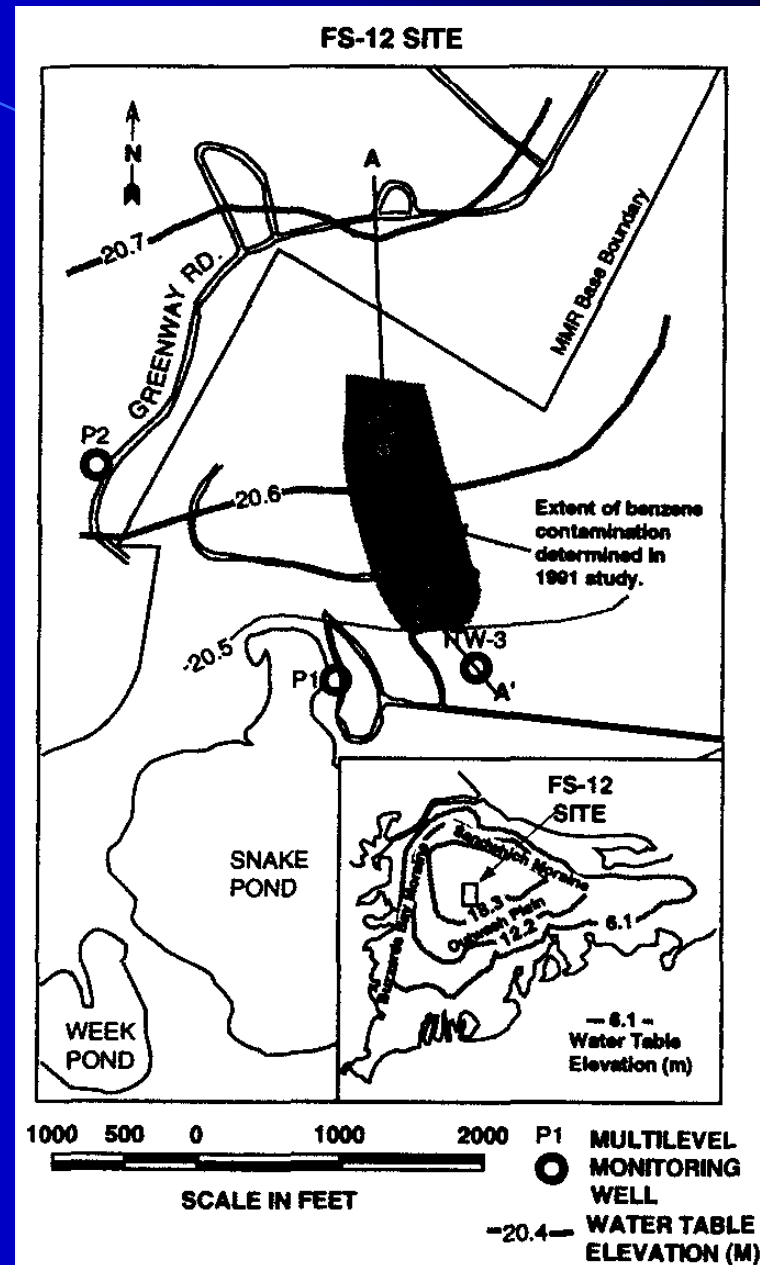


Figure 6-14. Plot of PO_4^{3-} versus NO_3^- in water samples from feedlot runoff (M), cultivated fields (F), uncontaminated groundwater (G), and contaminated well water (W). The sample of contaminated well water falls within the triangle defined by compositions M, G, and F, indicating that this sample is a mixture of these three compositions. The relative proportions of each end member can be determined by applying the lever rule (see Example 6-11).

Figure 6-C1-1. Location and extent of spill. From "Site Characterization using 3H/3He Ground Water Ages, Cape Cod, MA" by D. K. Solomon, R. J. Poreda,, P. G. Cook and A. Hunt, GROUND WATER; Vol.33, No. 6, p. 989 (Figure 1, FS 12). November/December 1995. Reprinted from GROUND WATER with permission of the National Ground Water Association. Copyright 1995.



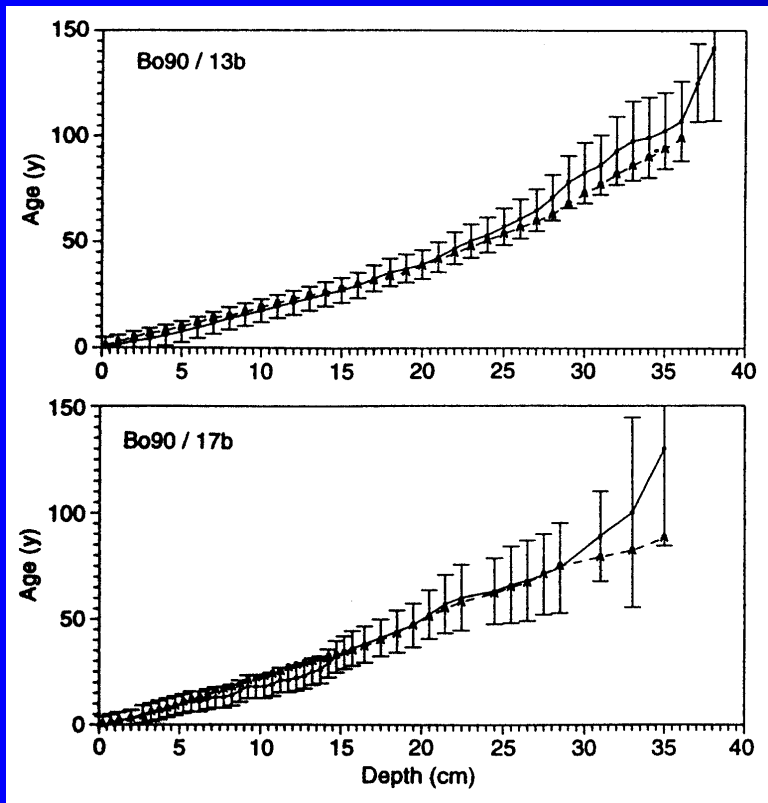


Figure 6-C2-1. ^{210}Pb ages for the two cores using a constant-flux model (solid line) compared to lamination counting (dashed line). From Bollhöfer et al. (1994).

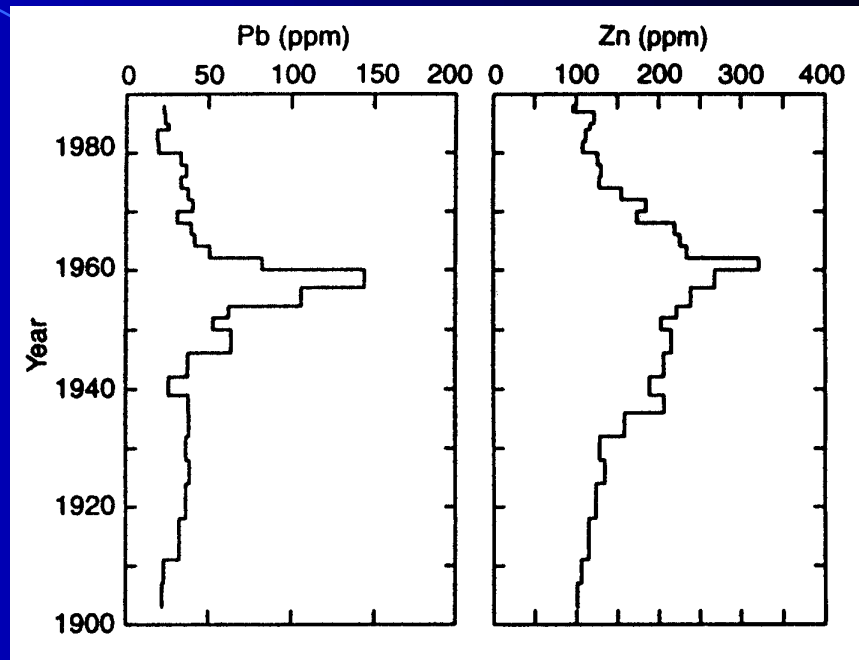


Figure 6-C2-2. Lead and zinc concentrations versus ^{210}Pb age in sediment core 13b. From Bollhöfer et al. (1994).

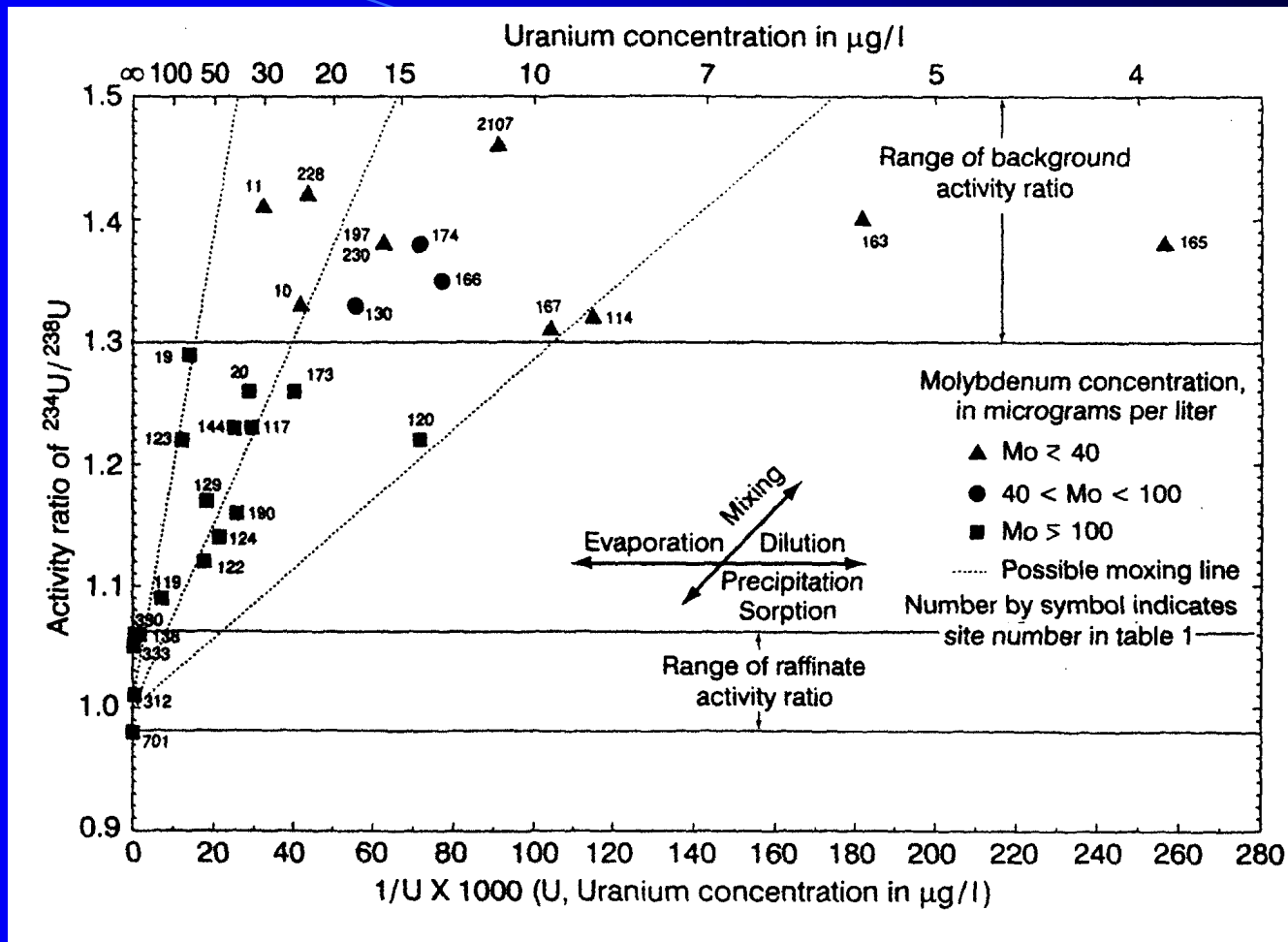


Figure 6-C3-1. Relationship between AR and U content of groundwater samples and raffinate. The effect of various processes on these values is illustrated in the figure. Evaporation and dilution (or sorption) will change the total uranium concentration. Only mixing will change the AR values. From Zielinski et al. (1997).

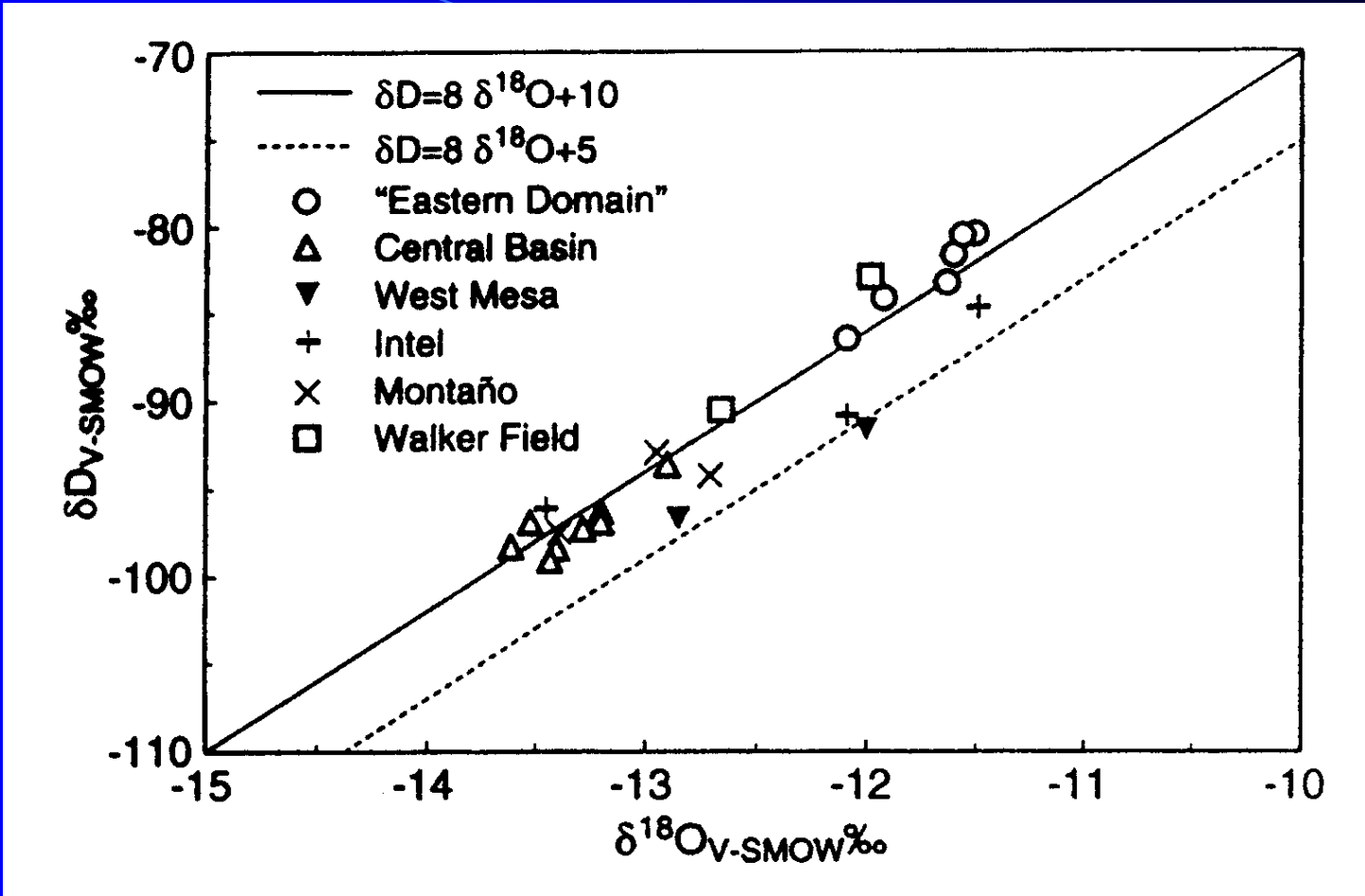


Figure 6-C4-1. δD and $\delta^{18}O$ for various groundwaters from the Albuquerque Basin showing the various groundwater domains. From Lambert and Balsley (1997).

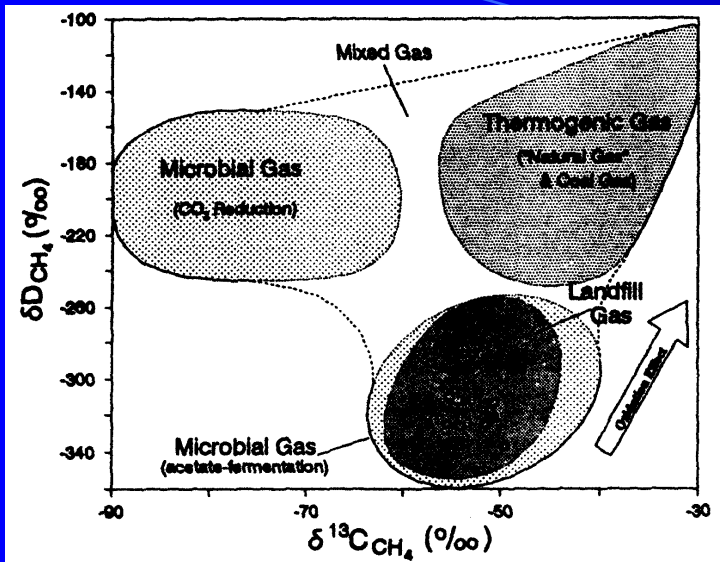


Figure 6-C5-1. δD versus $\delta^{13}C$ for methane from different sources. Landfill methane plots in the field of acetate-fermentation.*

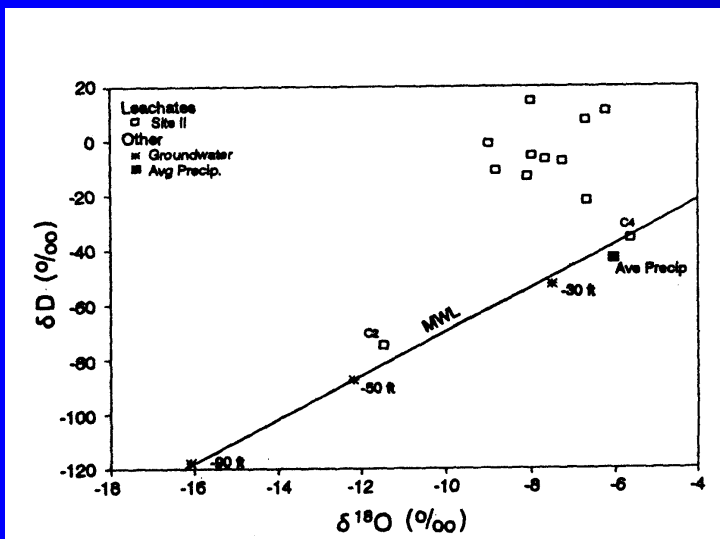


Figure 6-C5-2. δD versus $\delta^{18}O$ for leachates from a municipal landfill in Illinois. The leachates are relatively enriched in deuterium compared to meteoric water. The two leachate samples (C2 and C4) that fall on the meteoric water line (MWL) represent leachate significantly diluted by precipitation (C2) or from a recent precip portion of the landfill (C4).*

*Source: From "Environmental Isotope Characteristics of Landfill Leachates and Gases" by K. C. Hackley, C. L. Lui and D. D. Coleman, GROUND WATER; Vol. 34, No. 5, pp. 831-834 (Figures 5, 8, 9). September/October 1996. Reprinted from GROUND WATER with permission of the National Ground Water Association. Copyright 1996.

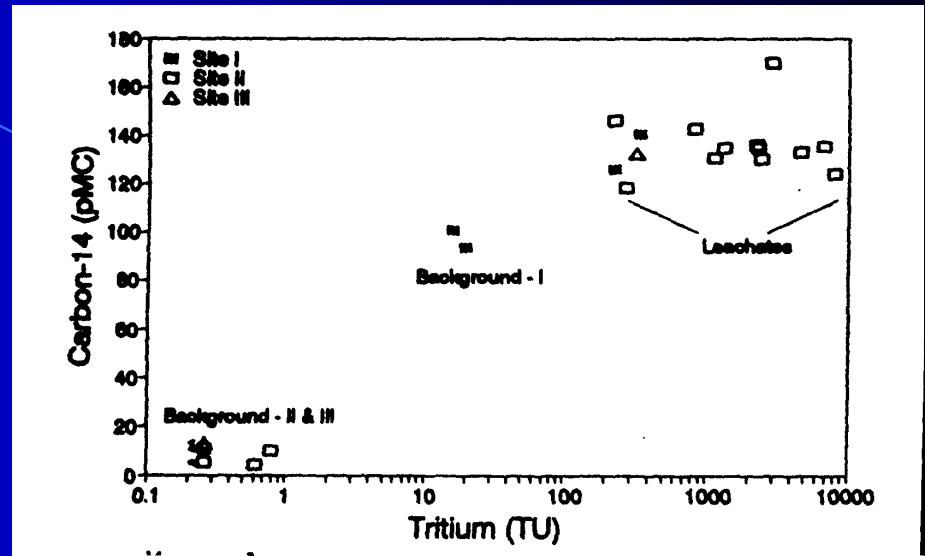


Figure 6-C5-3. ^{14}C and 3H activities for leachates from three Illinois landfills. Background-I was determined from surface and shallow groundwater. Backgrounds-II and -III were determined for confined aquifers at a depth of 30 m. Background-I shows the influence of present-day bomb-derived radiogenic isotopes.*

Figure 6-C6-1. $\delta^{15}\text{N}$ values for groundwaters from various land-use areas. Forms of nitrogen applied to cultivated areas are shown on the diagram. From “Nitrogen Isotopes as Indicators of Nitrate Sources in Minnesota Sand-Plain Aquifers” by S. C. Komor and H. W. Anderson, *GROUND WATER*; Vol. 31, No. 2, p. 266 (Figure 3). March/April 1993. Reprinted from *GROUND WATER* with permission of the National Ground Water Association. Copyright 1993.

